THE JOURNAL OF BIOLOGICAL CHEMISTRY Vol. 279, No. 43, Issue of October 22, pp. 44987–44995, 2004
Printed in U.S.A.

Comparative Mechanistic and Substrate Specificity Study of Inositol Polyphosphate 5-Phosphatase *Schizosaccharomyces pombe* Synaptojanin and SHIP2*

Received for publication, June 9, 2004, and in revised form, August 13, 2004
Published, JBC Papers in Press, August 16, 2004, DOI 10.1074/jbc.M406416200

Yuling Chi‡§, Bo Zhou‡, Wei-Qing Wang‡, Sung-Kee Chung¶, Yong-Uk Kwon¶, Young-Hoon Ahn‖, Young-Tae Chang‖, Yosuke Tsujishita‡‡, James H. Hurley**, and Zhong-Yin Zhang‡¶¶**

*From the ‡Department of Molecular Pharmacology, Albert Einstein College of Medicine, Bronx, New York 10461, ¶Department of Chemistry, Pohang University of Science and Technology, Pohang 790-784, Korea, ‖Department of Chemistry, New York University, New York, New York 10003, and **Laboratory of Molecular Biology, NIDDK, National Institutes of Health, United States Department of Health and Human Services, Bethesda, Maryland 20892*

Inositol-5-phosphatases are important enzymes involved in the regulation of diverse cellular processes from synaptic vesicle recycling to insulin signaling. We describe a comparative study of two representative inositol-5-phosphatases, *Schizosaccharomyces pombe* synaptojanin (SPsynaptojanin) and human SH2 domain-containing inositol-5-phosphatase SHIP2. We show that in addition to Mg^{2+}, transition metals such as Mn^{2+}, Co^{2+}, and Ni^{2+} are also effective activators of SPsynaptojanin. In contrast, Ca^{2+} and Cu^{2+} are inhibitory. We provide evidence that Mg^{2+} binds the same site occupied by Ca^{2+} observed in the crystal structure of SPsynaptojanin complexed with inositol 1,4-bisphosphate ($Ins(1,4)P_2$). Ionizations important for substrate binding and catalysis are defined for the SPsynaptojanin-catalyzed $Ins(1,4,5)P_3$ reaction. Kinetic analysis with four phosphatidylinositol lipids bearing a 5-phosphate and 54 water-soluble inositol phosphates reveals that SPsynaptojanin and SHIP2 possess much broader substrate specificity than previously appreciated. The rank order for SPsynaptojanin is $Ins(2,4,5)P_3$ > phosphatidylinositol-4,5-bisphosphate ($PtdIns(4,5)P_2$) ≈ $Ins(4,5)P_2$ ≈ $Ins(1,4,5)P_3$ ≈ $Ins(4,5,6)P_3$ > $PtdIns(3,5)P_2$ ≈ $PtdIns(3,4,5)P_3$ ≈ $Ins(1,2,4,5)P_4$ ≈ $Ins(1,3,4,5)P_4$ ≈ $Ins(2,4,5,6)P_4$ ≈ $Ins(1,2,4,5,6)P_5$. The rank order for SHIP2 is $Ins(1,2,3,4,5)P_5$ > $Ins(1,3,4,5)P_4$ > $PtdIns(3,4,5)P_4$ ≈ $PtdIns(3,5)P_2$ ≈ $Ins(1,4,5,6)P_4$ ≈ $Ins(2,4,5,6)P_4$. Because inositol phosphate isomers elicit different biological activities, the extended substrate specificity for SPsynaptojanin and SHIP2 suggest that these enzymes likely have multiple roles in cell signaling and may regulate distinct pathways. The unique substrate specificity profiles and the importance of 2-position phosphate in binding also have important implications for the design of potent and selective SPsynaptojanin and SHIP2 inhibitors for pharmacological investigation.

Eukaryotic cells contain both water-soluble inositol phosphates and the corresponding phosphoinositide lipids. These molecules reside in different cellular compartments and regulate the localization and activity of proteins through their interaction with specific binding domains. Inositol and phosphatidylinositol phosphates are key modulators of cellular processes including signal transduction, cell proliferation, and apoptosis, vesicle trafficking, cell motility and cytoskeletal organization, and transcription (1–5). The best known inositol-based signaling pathway is the cell surface receptor-triggered hydrolysis of phosphatidylinositol 4,5-bisphosphate ($PtdIns(4,5)P_2$)[1] by phospholipase C to yield the second messengers inositol 1,4,5-triphosphate ($Ins(1,4,5)P_3$), a regulator of Ca^{2+} release, and diacylglycerol, an activator of protein kinase C. The activity of the inositol-based molecules depends on which site(s) on the inositol ring is phosphorylated, and the level of phosphorylation is maintained by the combined action of a host of inositol kinases and phosphatases. Although considerable effort has been directed toward the analysis of the kinases that produce the phosphorylated inositol molecules, the study of phosphatases that oppose the activity of these kinases remains limited.

There are several distinct families of inositol phosphatases that are capable of removing the phosphoryl group from the inositol ring (3, 6). The inositol phosphatases are classified according to the position of the phosphate that they hydrolyze. For instance, dephosphorylation of the D1 position is carried out by the inositol polyphosphate 1-phosphatase, which is a member of an Mg^{2+}-dependent, Li^{+}-inhibited gene family (7). The hydrolysis of the D3 phosphate is catalyzed by the inositol polyphosphate-3-phosphatases that include the tumor suppressor PTEN and the myotubularin family of phosphatases (6). PTEN and myotubularins have the same active site sequence CX_5R that characterize the protein-tyrosine phosphatase superfamily (8). Interestingly, the newly identified inositol polyphosphate 4-phosphatases responsible for the hydrolysis of the D4 phosphate also contain the CX_5R catalytic motif (9). Finally, the removal of the D5 phosphate is accomplished by a large family of inositol polyphosphate-5-phosphatases, which

* This work was supported by National Institutes of Health Grant CA69202 and the G. Harold and Leila Y. Mathers Charitable Foundation. The costs of publication of this article were defrayed in part by the payment of page charges. This article must therefore be hereby marked "*advertisement*" in accordance with 18 U.S.C. Section 1734 solely to indicate this fact.

§ Supported in part by National Institutes of Health Grant Training Grant 5T32-CA09475.

‡‡ Current address: Department of Psychiatry, Nanzan Hospital, Okinawa, Japan.

¶¶ To whom correspondence should be addressed: Dept. of Molecular Pharmacology, Albert Einstein College of Medicine, 1300 Morris Park Ave., Bronx, NY 10461. Tel.: 718-430-4288; Fax: 718-430-8922; E-mail: zyzhang@aecom.yu.edu.

[1] The abbreviations used are: $PtdIns(4,5)P_2$, phosphatidylinositol 4,5-bisphosphate; $Ins(1,4)P_2$, inositol 1,4-bisphosphate; $Ins(1,4,5)P_3$, inositol 1,4,5-trisphosphate; $Ins(1,3,4,5)P_4$, inositol 1,3,4,5-tetrakisphosphate; $Ins(1,2,3,4,5)P_5$, inositol 1,2,3,4,5-pentakisphosphate; $PtdIns(3,5)P_2$, phosphatidylinositol 3,5-bisphosphate; $PtdIns(3,4,5)P_3$, phosphatidylinositol 3,4,5-trisphosphate; SHIP, SH2-containing inositol-5-phosphatase; SPsynaptojanin, synaptojanin from *S. pombe*; TOCSY, total correlation spectroscopy; $diC_4PtdIns$, D(+)-*sn*-1,2-di-*O*-butanoylglycerol, 3-*O*-phospho-linked inositol.

can be further classified into type I enzymes that hydrolyze only water-soluble substrates, type II enzymes that hydrolyze both water-soluble and lipid substrates, type III enzymes that hydrolyze only substrates with a 3-position phosphate, and type IV enzymes that are poorly characterized and are active only toward PtdIns(3,4,5)P_3 (3, 10). The crystal structure of a type II 5-phosphatase SPsynaptojanin has been determined, revealing a fold similar to metal-dependent endonucleases (11).

Recent studies have documented the critical roles of inositol polyphosphate-5-phosphatases in normal physiology and disease. The synaptojanin-catalyzed dephosphorylation of PtdIns(4,5)P_2 is essential for proper synaptic vesicle recycling (12). The insulin-stimulated production of PtdIns(3,4,5)P_3 is central to glucose homeostasis. Mice deficient of SHIP2, an SH2 domain-containing inositol-5-phosphatase that dephosphorylates PtdIns(3,4,5)P_3, are hypoglycemic and sensitized to insulin, suggesting that SHIP2 may be a potential therapeutic target for the treatment of type II diabetes (13). Certain human diseases are also associated with genetic mutations affecting the 5-phosphatase activity. The Lowe oculocerebrorenal syndrome is an X-linked disorder characterized by congenital cataracts, mental retardation, and renal Fanconi syndrome. The oculocerebrorenal gene encodes a 5-phosphatase that exhibits diminished enzyme activity in oculocerebrorenal patients (14).

Elucidating the molecular determinants for inositol polyphosphate-5-phosphatase catalysis and substrate specificity is crucial to our understanding of how this family of enzymes regulates cellular signaling. In the following we describe two convenient, non-radioactive methods for assaying inositol phosphatase activity. We report a detailed kinetic analysis of the reaction catalyzed by a putative mammalian synaptojanin homologue from *Schizosaccharomyces pombe* (SPsynaptojanin) with regard to metal ion and pH dependence. SPsynaptojanin was chosen as a model system since it is the only 5-phosphatase with a known crystal structure. To provide further insight into the function of 5-phosphatases, we also describe an investigation of SPsynaptojanin and SHIP2 substrate specificity with more than 50 water-soluble and lipid inositol phosphates. SHIP2 was chosen as a subject of study because of its importance in insulin signaling and its potential as a therapeutic target. Knowledge of the substrate specificity of inositol-5-phosphatases may shed new light on the roles played by these enzymes in cellular physiology and furnish valuable information for the design of potent small molecule inhibitors for biological studies and therapeutic development.

EXPERIMENTAL PROCEDURES

Materials—Ins(1,5)P_2, Ins(1,3,5)P_3, Ins(1,3,4,5)P_4, diC_4PtdIns(5)P, diC_4PtdIns(4,5)P_2, diC_4PtdIns(3,5)P_2, and diC_4PtdIns(3,4,5)P_3 were purchased from Echelon (Salt Lake City, UT). Ins(1,4,5)P_3 and purine nucleoside phosphorylase were purchased from Sigma. All other inositol phosphates were synthesized as described (15–21). It should be noted that InsP_1s and InsP_2s are racemic mixtures, whereas other inositol phosphates (InsP_3s, InsP_4s, and InsP_5s) are chirally pure.

Mutagenesis—The SPsynaptojanin mutants were constructed with the QuikChange site-directed mutagenesis kit from Stratagene using a pET22b plasmid containing the coding sequence for the SPsynaptojanin 5-phosphatase domain (residues 534–880) (11). Mutations were confirmed by DNA sequencing.

Expression and Purification of SPsynaptojanin and SHIP2—The inositol polyphosphate-5-phosphatase domain (Ipp5c) of SPsynaptojanin was constructed into the pET22b vector with a His_6 tag and a tobacco etch virus protease site at its N terminus. The plasmid was transformed into BL21/DE3 competent cells by standard procedure. A single colony was selected and grown in LB medium (supplemented with 100 μg/ml ampicillin) at 37 °C overnight. A 10-ml overnight culture was transferred to 1 liter of LB medium (supplemented with 100 μg/ml ampicillin) and allowed to grow at 37 °C until the absorbance at 600 nm was 0.6–0.8. Isopropyl-1-thio-β-D-galactopyranoside (1 mM) was added to induce SPsynaptojanin expression. After further incubation at room temperature with shaking for 16 h, the cells were harvested by centrifugation at 5000 rpm for 5 min. The cell pellet from 1 liter of culture was resuspended in 30 ml of lysate buffer (20 mM Tris-HCl, pH 7.9, 500 mM NaCl, 5 mM imidazole). The cells were lysed by passage through a French press at 12,000 p.s.i. twice. Cellular debris was removed by centrifugation at 16,000 rpm for 30 min. A 2-ml 50% slurry of nickel nitrilotriacetic acid-agarose (Qiagen) was equilibrated with lysate buffer and added to the lysate supernatant. After incubation with gentle agitation at 4 °C for 1 h, the matrix was transferred into a column and washed with 20 ml of lysate buffer. The His_6-tagged protein was eluted by buffers containing concentrations of imidazole of 5, 20, 50, and 110 mM in 20 mM Tris-HCI, pH 7.9, 500 mM NaCl. Fractions containing SPsynaptojanin were pooled together and concentrated with a Centriprep-30 filtration unit (Amicon). Mutants were further purified by fast protein liquid chromatography with a Superdex G-75 column using an elution buffer containing 50 mM Tris, pH 7.9, 300 mM NaCl. Protein purity was checked by 10% SDS-PAGE. Protein concentration was determined by a Bio-Rad protein assay.

The SHIP2 catalytic domain (residues 419–732) was constructed into the pET22b vector, with a His_6 tag and a tobacco etch virus protease site at its N terminus. The plasmid was transformed into BL21/DE3 competent cell by standard procedure. A 10-ml overnight culture was transferred to 1 liter of LB medium (supplemented with 100 μg/ml ampicillin) and allowed to grow at 37 °C until the absorbance at 600 nm was 0.6. Without the addition of isopropyl-1-thio-β-D-galactopyranoside, the culture was incubated at room temperature with shaking for an additional 6 h. The cells were harvested by centrifugation at 5000 rpm for 5 min. The cell pellets from 1 liter of culture was resuspended in 30 ml of lysate buffer (20 mM Tris-HCl pH 7.9, 500 mM NaCl, 5 mM imidazole). The cells were lysed by passage through a French press cell at 12,000 p.s.i. twice. Cellular debris was removed by centrifugation at 16,000 rpm for 30 min. A 2-ml 50% slurry of nickel nitrilotriacetic acid-agarose (Qiagen) was equilibrated with the lysate buffer and added to the lysate supernatant. After incubating with gentle agitation at 4 °C for 1 h, the matrix was transferred into a column and washed with 20 ml of lysate buffer. The His_6-tagged protein was eluted by an imidazole gradient from 5 to 150 mM in 20 mM Tris-HCI, pH 7.9, 500 mM NaCl. Fractions the SHIP2 protein were pooled together and concentrated with a Centriprep-30 filtration unit (Amicon), and the buffer was changed to 25 mM Tris-HCl, pH 7.5, 1 mM EDTA, 1 mM dithiothreitol. The purified protein was made to 20% glycerol and stored at −80 °C.

Ammonium Molybdate Inorganic Phosphate Assay—In a typical assay (22) the inositol phosphate was incubated at 30 °C in a buffer containing 50 mM HEPES, 100 mM NaCl, 1 mM $MgCl_2$, with or without 0.25 mM EDTA at pH of 7.4 for 10 min. To determine the steady state kinetic parameters K_m and k_{cat}, the substrate concentrations were in the range of 3–300 μM. For activity comparison, the concentrations of inositol phosphates were fixed at 200 μM. To ensure initial rate conditions, the product *versus* time progress curves were routinely checked for linearity at different substrate and enzyme concentrations. In all cases the enzyme concentration was at least 100-fold lower than that of the substrate, and the quantity of substrate consumed was less than 10% of the initial value, so that the steady state assumption was fulfilled. There was no product inhibition under these conditions. Reactions were started by the addition of an appropriate amount of SPsynaptojanin (4 μl) to the reaction mixture containing the substrate (100 μl). After an appropriate amount of time, usually 5 min, 25 μl of 10% (w/v) trichloroacetic acid was used to quench the reaction. Then, 65 μl of solution B was added to the mixture. 2.5 min later solution C was added. The reaction mixture was well mixed every time after the addition of reagents. UV-visible absorbance at 700 nm was measured 5 min after final mix. Here, solution B is a mixture of 3.4 ml of 2% (w/v) ammonium molybdate and 1 g of L-ascorbic acid in 4.9 ml of 50% trichloroacetic acid and made freshly daily. Solution C contains 2% (w/v) sodium arsenite in 2% (v/v) acetic acid. The measurements of activity in the absence of EDTA were conducted in the same buffer, except there was no EDTA.

Continuous Spectrophotometric Enzyme-coupled Assay—Kinetic parameters for the dephosphorylation of inositol phosphate were also determined using a continuous spectrophotometric assay. This assay incorporates a coupled enzyme system, which uses purine nucleoside phosphorylase and its chromogenic substrate 7-methyl-6-thioguanosine for the quantification of inorganic phosphate produced in the phosphatase reaction (23, 24). The change in absorbance at 360 nm was due to the conversion of 7-methyl-6-thioguanosine to 7-methyl-6-thioguanine in the presence of inorganic phosphate. Quantitation of the inorganic phosphate produced in the phosphatase reaction was determined using the extinction coefficient of 11,200 M^{-1} cm^{-1} at 360 nm and pH 7.0.

Experiments were carried out at 30 °C in a 1.6-ml reaction mixture containing 100 mM NaCl, 50 mM HEPES, 1 mM Mg^{2+}, 0.25 mM EDTA, pH 7.4, 0.1 mg/ml purine nucleoside phosphorylase (Sigma), and 200 μM 7-methyl-6-thioguanosine. The spectrophotometric measurements were conducted using a PerkinElmer Life Sciences Lambda 14 spectrophotometer equipped with a magnetic stirrer in the cuvette holder.

NMR Measurements—0.6 ml of 1.5 mM Ins(1,4,5)P_3 was dissolved in a buffer containing 100 mM NaCl, 50 mM deuterated Tris, 1 mM $MgCl_2$, 0.25 mM EDTA in D_2O at pH 7.1. The spectra for Ins(1,4,5)P_3 both before and after the addition of SPsynaptojanin were acquired. NMR experiments were performed at 26 °C on a Bruker DRX 300 spectrometer. Phosphorus chemical shifts were relative to an external standard (85% phosphoric acid) set at 0.0 ppm. Two-dimensional ^{1}H-^{1}H total correlation spectroscopy (TOCSY) spectra were collected using an 80-ms MLEV-17 spin lock and WATERGATE water suppression with 4000 and 256 points in F2 and F1, respectively, with 16 scans per t_1 point and a recycle delay of 1.5 s. The experiments used a proton sweep width of 14 ppm with the carrier set to 4.7 ppm. Spectra were processed with a cosine bell window function and zero-filled to yield data sets with 4000 and 512 points in F2 and F1, respectively. ^{31}P-Decoupled two-dimensional ^{1}H-^{1}H TOCSY spectra were collected as above and used GARP ^{31}P-decoupling during the acquisition period. Proton chemical shifts were referenced to 3-(trimethylsilyl)propionate. Proton coupled and decoupled ^{31}P NMR spectra were collected at 121.5 MHz, with an acquisition time of 1.347 s, and 512 transition scans.

RESULTS AND DISCUSSION

Characterization of SPsynaptojanin as an Inositol Polyphosphate-5-phosphatase—Recently, the crystal structure of a previously uncharacterized putative mammalian synaptojanin homologue from *S. pombe* (SPsynaptojanin) was reported (11). This was the first three-dimensional structure of a catalytic domain from the inositol-5-phosphatase family. This structure was solved after soaking the crystals of SPsynaptojanin for 20 h in 2 mM Ins(1,4,5)P_3 and 1 mM $CaCl_2$. The electron difference density indicated that the putative hydrolysis product Ins(1,4)P_2, not Ins(1,4,5)P_3, was bound at the active site. Given the fact that the catalytic domain of SPsynaptojanin shows significant sequence identity to those of mammalian inositol polyphosphate-5-phosphatases, the presence of Ins(1,4)P_2 in the active site is consistent with the expectation that SPsynaptojanin is an inositol-5-phosphatase.

To further characterize the regiospecificity of SPsynaptojanin for the 5 position of Ins(1,4,5)P_3, NMR measurements were conducted on a reaction containing SPsynaptojanin and Ins(1,4,5)P_3 to identify the position(s) of dephosphorylation. The ^{1}H-coupled ^{31}P NMR spectrum of the starting material Ins(1,4,5)P_3 shows that there are three phosphorus peaks, each split by one proton, consistent with the three phosphates attached to the inositol ring (Fig. 1*Aa*). Fig. 1*Ab* is the corresponding ^{1}H-decoupled ^{31}P spectrum of Ins(1,4,5)P_3. Upon the addition of SPsynaptojanin, distinct spectral changes (Fig. 1*A*, *c* to *e*) occurred consistent with the disappearance of Ins(1,4,5)P_3 and the coincident appearance of a second set of peaks. Fig. 1*Af* is the ^{1}H-coupled ^{31}P NMR spectrum for the reaction upon prolonged incubation with SPsynaptojanin, which shows two peaks apparently split by a proton and a third peak that is insensitive to proton coupling, consistent with a single inositol bisphosphate and inorganic phosphate as the products of the reaction. To provide evidence that the inositol bisphosphate produced in the SPsynaptojanin-catalyzed Ins(1,4,5)P_3 reaction is Ins(1,4)P_2, we also collected the ^{31}P NMR spectra of authentic Ins(1,4)P_2 under identical conditions (Fig. 1*B*). Spectral comparison (Fig. 1, *A*, *e* and *f*, and *B*, *a* and *b*) suggests that the inositol bisphosphate produced in the SPsynaptojanin reaction is Ins(1,4)P_2.

The regiochemistry of the inositol bisphosphate produced in the SPsynaptojanin-catalyzed dephosphorylation of Ins (1,4,5)P_3 was further confirmed by ^{1}H TOCSY measurements. The overlay of the ^{31}P coupled (*black*) and decoupled (*red*) ^{1}H

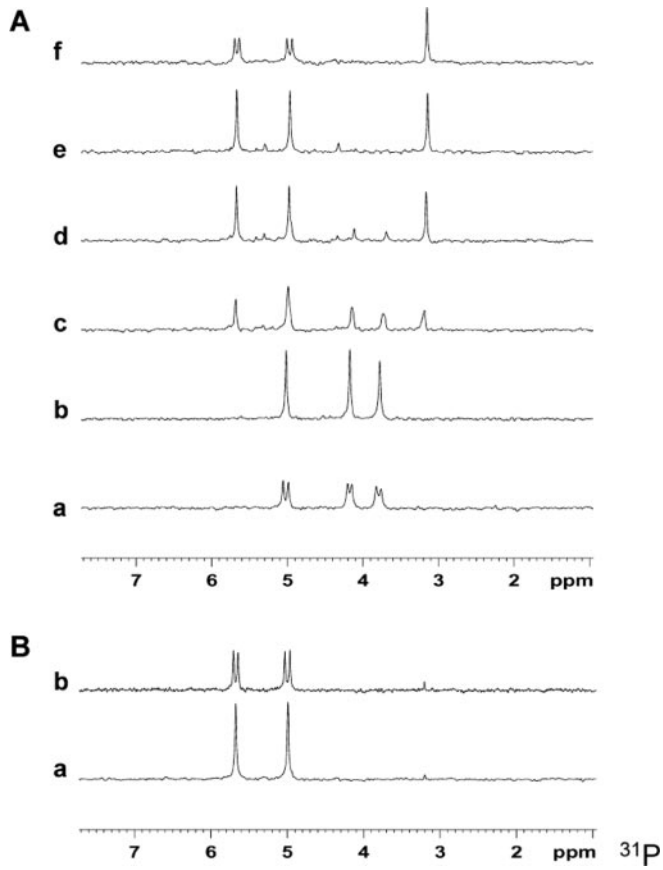

FIG. 1. **^{31}P NMR spectra of Ins(1,4,5)P_3 and Ins(1,4)P_2.** *A*: *a*, Ins(1,4,5)P_3 with ^{1}H coupling; *b*, Ins(1,4,5)P_3 without ^{1}H coupling; *c–e*, Ins(1,4,5)P_3 without ^{1}H coupling after SPsynaptojanin was added, and acquisitions were accumulated every 40 min. *f*, products of Ins(1,4,5)P_3 dephosphorylation by SPsynaptojanin with ^{1}H coupling. *B*: *a*, and *b*, Ins(1,4)P_2 without and with ^{1}H coupling, respectively.

TOCSY spectra shows that the inositol phosphate product has two phosphates that are linked at the 1 and 4 positions of inositol (Fig. 2), based upon the previous one-dimensional ^{1}H NMR spectral assignments of Ins(1,4)P_2 (25). Collectively, the NMR results establish that the inositol phosphate product observed in the SPsynaptojanin-catalyzed Ins(1,4,5)P_3 reaction is Ins(1,4)P_2, in accord with the classification of SPsynaptojanin as a 5-phosphatase.

Non-radioactive Spectroscopic Assays for Inositol 5-Phosphatases—Traditionally, inositol-5-phosphatases are assayed with radioisotope-labeled substrates followed by chromatographic separation of the products from the substrates. Having established the regiospecificity of SPsynaptojanin, we set out to develop non-radioactive colorimetric procedures that would be more suitable for detailed mechanistic investigation and substrate specificity analysis. Because there are no significant absorbance or fluorescence spectral changes associated with the dephosphorylation of inositol phosphates, our assays have been focused on the determination of inorganic phosphate produced in the reaction. In this regard we adopted two methods for inorganic phosphate determination to measure inositol-5-phosphatase activity. The first method relies on the use of an ammonium molybdate reagent that reacts with inorganic phosphate to produce a bright blue color at 700 nm (22). No interference was observed with various inositol phosphates. With this assay, the steady state kinetic parameters k_{cat} and K_m for the SPsynaptojanin-catalyzed dephosphorylation of Ins(1,4,5)P_3 were determined to be 11.2 ± 0.4 s^{-1} and 57.8 ± 3.2 μM, respectively, at pH 7.4 and 30 °C (Fig. 3*A*). The second

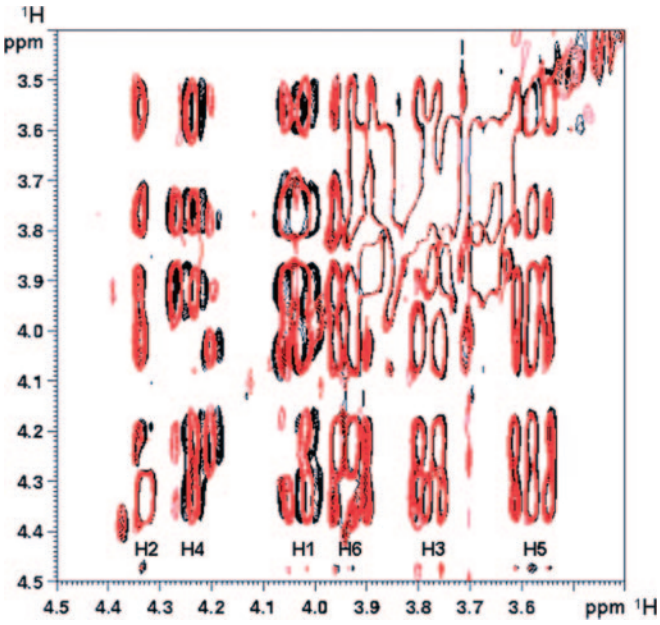

FIG. 2. **^{1}H TOCSY of the product of Ins(1,4,5)P_3 dephosphorylation with (*red*) and without (*black*) ^{31}P decoupling.** Chemical shifts of H1, H2, H3, H4, H5, and H6 were assigned according to Cerdan *et al.* (25).

method for the quantitation of inorganic phosphate is a continuous spectrophotometric enzyme-coupled assay in which the coupling enzyme, purine nucleoside phosphorylase, uses the inorganic phosphate, generated by the action of the 5-phosphatase, to convert 7-methyl-6-thioguanosine to 7-methyl-6-thioguanine and ribose-1-phosphate, resulting in an increase in absorbance at 360 nm (23). With the continuous coupled assay, the k_{cat} and K_m values for the same reaction under identical conditions were determined to be 11.0 ± 0.2 s^{-1} and 55.7 ± 2.9 μM, respectively (Fig. 3*B*). Thus, there is excellent agreement between these two methods, which allows some flexibility in assay choices and eliminates the need for radioactivity.

Metal Ion Dependence—It is known that inositol-5-phosphatases are Mg^{2+}-dependent phosphomonoesterases (3, 10). As expected, SPsynaptojanin displays no measurable activity in the absence of metal ions. The effect of Mg^{2+} concentration on the SPsynaptojanin reaction at 200 μM Ins(1,4,5)P_3 is shown in Fig. 4. As the concentration of Mg^{2+} is raised, the activity of SPsynaptojanin increases to a maximum at 2 mM metal ion concentration. Further increase in Mg^{2+} concentration leads to a decline in SPsynaptojanin activity, suggesting the existence of a second metal ion binding site that is inhibitory. Fitting the initial rate *versus* [Mg^{2+}] to Equation 1, which includes the inhibitory term, yielded the k_{cat}, K_m, and K_i values for Mg^{2+}. As listed in Table I, the K_m for Mg^{2+} is 530 μM, which is 16-fold lower than the K_i value, consistent with the fact that the binding of Mg^{2+} to the second inhibitory metal binding site is much weaker than the activation site.

$$v = k_{cat}[E]/(1 + K_m/[Mg^{2+}] + [Mg^{2+}]/K_i) \quad \text{(Eq. 1)}$$

To explore whether other divalent cations are also effective in activating SPsynaptojanin, we examined the effect of Ca^{2+}, Mn^{2+}, Co^{2+}, Ni^{2+}, and Cu^{2+} on the enzyme-catalyzed dephosphorylation of Ins(1,4,5)P_3. We found that neither Ca^{2+} nor Cu^{2+} was able to activate SPsynaptojanin. In contrast, transition metal ions Mn^{2+}, Co^{2+}, and Ni^{2+} were all activators of SPsynaptojanin. In addition, Mn^{2+}, Co^{2+}, and Ni^{2+} exhibited similar metal ion dependence on the SPsynaptojanin reaction as observed for Mg^{2+}, *i.e.* enzyme activity increased as a function of metal ion concentration to a maximum, after which additional metal ion led to enzyme inhibition (data not shown). The kinetic parameters for these metal ions are summarized in Table I. It appears that Mn^{2+}, Co^{2+}, Ni^{2+}, and Mg^{2+} can activate SPsynaptojanin to the same extent at saturating metal ion concentrations. However, the K_m values of Mn^{2+}, Co^{2+}, and Ni^{2+} for SPsynaptojanin are 30–80-fold lower than that of Mg^{2+}. Despite the higher affinities exhibited by Mn^{2+}, Co^{2+}, and Ni^{2+}, these metal ions are unlikely to be physiological relevant because cellular concentrations of free transition metals are significantly lower than those (6–15 μM) required for SPsynaptojanin activation. In contrast, the K_m for Mg^{2+} (530 μM) is within the physiological range, and thus, Mg^{2+} is likely the co-catalyst for SPsynaptojanin inside the cell.

Finally, we noted that although Mg^{2+} is absolutely required for SPsynaptojanin activity, sub-stoichiometric amounts of EDTA in the reaction could further enhance the 5-phosphatase activity. For example, when activity measurements were made in 50 mM HEPES buffer containing 100 mM NaCl, 1 mM Mg^{2+}, and 200 μM Ins(1,4,5)P_3, maximal SPsynaptojanin activity was observed at 0.25 mM EDTA (Fig. 5*A*). This rate-enhancing effect by EDTA may indicate the presence of inhibitory substances in the assay system, most likely trace amounts of heavy metals such as Cu^{2+}. Indeed, as shown in Fig. 5*B*, Cu^{2+} caused a concentration-dependent decrease in the 5-phosphatase activity in the presence of 1 mM Mg^{2+}, and the presence of 10 μM Cu^{2+} could completely abolish the Mg^{2+}-dependent 5-phosphatase activity. The addition of 0.25 mM EDTA to the reaction fully restored the SPsynaptojanin activity. Thus, unless stated otherwise, all assay systems contained 0.25 mM EDTA to sequester the inhibitory heavy metals in the buffer.

The Primary Metal Ion Binding Site in SPsynaptojanin—The x-ray crystal structure of SPsynaptojanin in complex with Ca^{2+} and Ins(1,4)P_2 reveals a Ca^{2+} binding site in the vicinity of the 4-phosphate group in Ins(1,4)P_2 (11). The bound Ca^{2+} is directly coordinated by three ligands from SPsynaptojanin and four water molecules (Fig. 6). Both carboxylate oxygens of Glu-597 and the amide oxygen of Asn-568 participate in Ca^{2+} binding. Of the four water molecules, two form bridging interactions with the 4-phosphate of Ins(1,4)P_2, one with the side chain oxygens of Asp-566 and Asp-838 and one with the main chain carbonyl of Leu-601. Although the Ca^{2+} binding site is well defined, its significance to SPsynaptojanin catalysis is unclear because unlike Mg^{2+}, no activity was detected for SPsynaptojanin in the presence of Ca^{2+} at concentrations up to 8 mM. In fact, we found that Ca^{2+} is inhibitory to the Mg^{2+}-dependent activity, in agreement with an earlier observation with a different inositol-5-phosphatase (26). The Ca^{2+} inhibition constant and its mode of inhibition were determined by varying the Mg^{2+} concentration at fixed levels of Ca^{2+}. As shown in Fig. 7, the effect of Ca^{2+} on the Mg^{2+}-dependent SPsynaptojanin-catalyzed dephosphorylation of Ins(1,4,5)P_3 displayed the characteristic intersecting line pattern for competitive inhibition. The K_i value for Ca^{2+} inhibition is 668 ± 78 μM.

The fact that Ca^{2+} inhibits the SPsynaptojanin reaction competitively with respect to the Mg^{2+} co-factor suggests that they may compete for the same binding site. To test this hypothesis, we assessed the effect of structural perturbations to the Ca^{2+} binding site on SPsynaptojanin activity. Because both carboxylate oxygens of Glu-597 are involved in coordinating the Ca^{2+}, we chose to replace Glu-597 with either an Ala or Gln. The catalytic activity of the E597A and E597Q mutants were found to be 4 and 3 orders of magnitude lower than that of the wild-type enzyme at 1 mM Mg^{2+}, a concentration that fully activates the wild-type enzyme. To determine whether the lower activity for E597Q is a result of lost affinity for Mg^{2+}, we measured the Mg^{2+} concentration dependence of the E597Q-

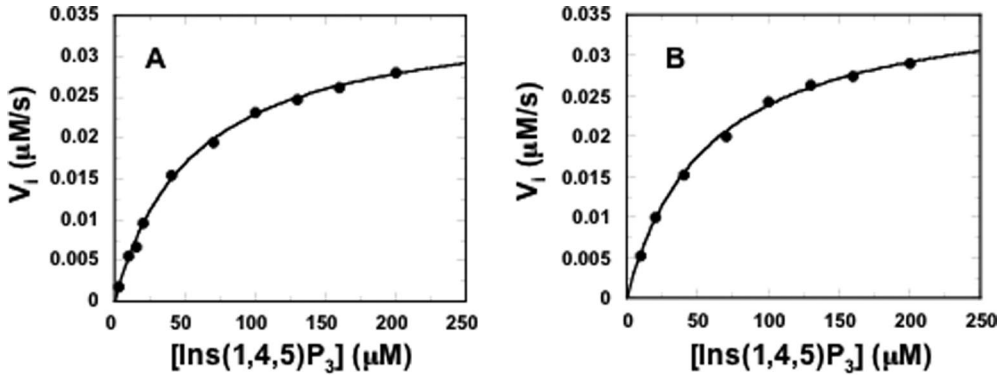

FIG. 3. **Steady state kinetic parameters obtained by nonlinear regression fit of the initial rate *versus* [S] to the Michaelis-Menten equation.** The initial rates were determined by the molybdate-inorganic phosphate colorimetric assay (*A*) and the continuous enzyme coupled assay (*B*).

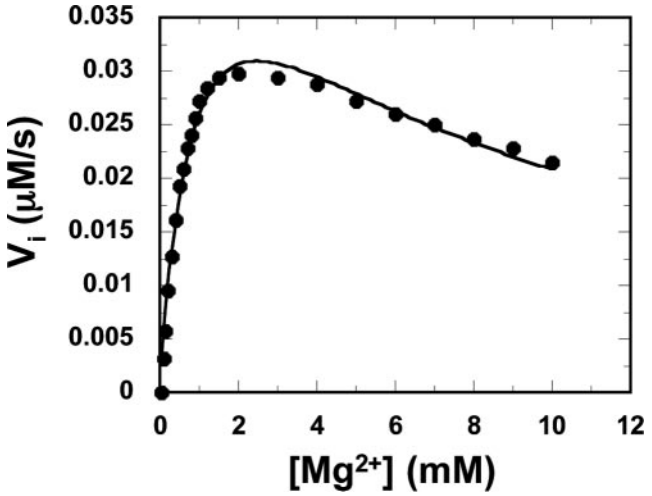

FIG. 4. **Mg^{2+} concentration dependence.** The concentration of SPsynaptojanin was 4.4 nM, and the concentration of Ins(1,4,5)P_3 was 200 μM. The theoretical curve was generated by nonlinear fit of the data to Equation 1.

TABLE I
SPsynaptojanin metal ion dependence

Metal ions	k_{cat}	K_m	K_i
	s^{-1}	μM	mM
Mg^{2+}	9.64 ± 0.60	530 ± 41	8.57 ± 0.76
Mn^{2+}	7.48 ± 0.30	12.0 ± 1.0	1.56 ± 0.17
Ni^{2+}	5.48 ± 0.34	6.39 ± 0.56	2.01 ± 0.12
Co^{2+}	7.28 ± 0.73	14.5 ± 1.1	3.25 ± 0.20

catalyzed Ins(1,4,5)P_3 dephosphorylation. The results indicated that the Mg^{2+} concentration obeys Michaelis-Menten saturation kinetics (data not shown). Kinetic analysis shows that the E597Q-catalyzed reaction displays a k_{cat} of 0.078 ± 0.002 s^{-1} and a K_m of 1.30 ± 0.14 mM for Mg^{2+}. Thus, replacement of the carboxylate at residue 597 by a carboxyamide causes a greater than 140-fold decrease in SPsynaptojanin catalytic efficiency, whereas the affinity for Mg^{2+} is reduced by only 2.4-fold. This result suggests that although Glu-597 is not essential for metal ion binding affinity, the precise interactions between the metal and Glu-597 may be more important for proper positioning and orientation of the metal ion relative to the reactive center for catalysis. The dramatic effects on the Mg^{2+}-dependent SPsynaptojanin activity observed as a result of a subtle change to the Ca^{2+} binding site provide further evidence that Mg^{2+} and Ca^{2+} bind to the same site.

The drastically different behaviors of Mg^{2+} and Ca^{2+} in enzyme catalysis are quite common. Ca^{2+} and Mg^{2+} belong to the same elemental group in the periodic table, and the main difference between the two metals is ionic size. Size variation of the metal ion can result in different coordination chemistries and spatial arrangements between the metal ion and the substrate, which could be either activating or inhibitory to enzyme activity. Thus, although Mg^{2+} and Ca^{2+} bind to the same site in SPsynaptojanin, their interactions with the enzyme and the substrate may be different. It is of interest to note that the free intracellular Ca^{2+} concentration in resting cells is very low, ~10–100 nM. In this concentration range, it is unlikely that Ca^{2+} will exert any influence on SPsynaptojanin activity. However, free Ca^{2+} concentration within the cell can rise up to the low millimolar range upon Ca^{2+} release from internal stores, which is triggered by the binding of Ins(1,4,5)P_3 to its receptors (27). At low millimolar concentrations, Ca^{2+} can effectively block the action of inositol-5-phosphatase, therefore potentially prolonging Ca^{2+} signaling.

pH-rate Profiles—To determine the ionization constants important for SPsynaptojanin catalysis and substrate binding, we obtained the k_{cat} and k_{cat}/K_m values using Ins(1,4,5)P_3 as a substrate at various pH values and 1 mM Mg^{2+} concentration. The k_{cat}/K_m parameter is the apparent second-order rate constant for the reaction of free enzyme and free substrate and includes the binding of substrate through the first irreversible step. The kinetic parameter k_{cat} describes the rate-limiting step under saturating concentrations of the substrate. Plots of k_{cat}/K_m *versus* pH yield critical pK_a values for free enzyme and/or substrate, which are essential for binding and/or catalysis, and plots of k_{cat} *versus* pH provide the essential pK_a values of the enzyme-substrate complex, whose decomposition is rate-limiting. The plot of k_{cat}/K_m *versus* pH (Fig. 8*A*) shows a bell-shaped curve with a maximum at pH 7.4 and with a limiting slope of +1 on the acidic side and −2 on the basic side. Thus, the k_{cat}/K_m *versus* pH profile for Ins(1,4,5)P_3 indicates that in the free enzyme or substrate, one group with a pK_a of 7.59 ± 0.65 must be deprotonated and two groups with a pK_a of 6.66 ± 0.12 and 8.41 ± 0.58, respectively, must be protonated for optimal catalysis. The plot of k_{cat} *versus* pH (Fig. 8*B*) also shows a bell-shaped curve with pH maximum of 7.2 and a slope of +1 on the acidic limb and −1 on the basic limb. The data indicate that two groups in the enzyme-substrate complex are involved in catalysis, one group with a pK_a value of 6.60 ± 0.10 must be deprotonated and one group with a pK_a value of 7.75 ± 0.08 must be protonated. Because several groups in the enzyme and substrate can ionize in the pH range of 6–8.5, the identities of the critical ionizations for k_{cat}/K_m and k_{cat} will require further investigation.

Substrate Specificity of SPsynaptojanin and SHIP2—There are currently four known substrates for 5-phosphatases:

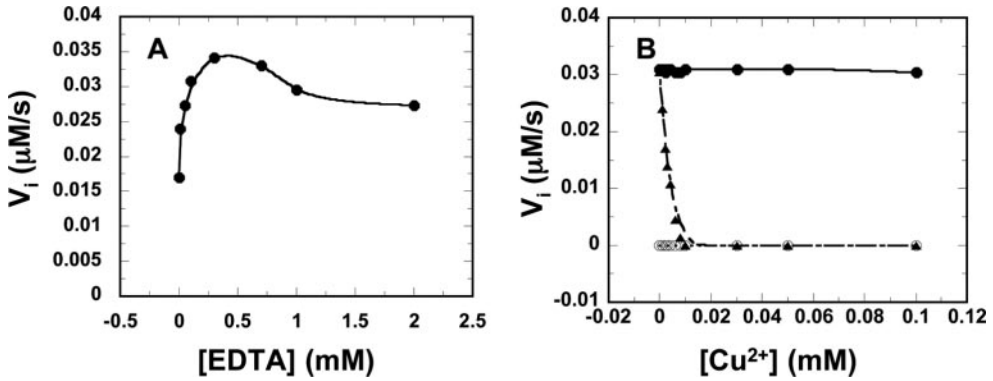

FIG. 5. **Effect of EDTA and heavy metal ion Cu^{2+}.** *A*, EDTA effect on the catalytic activity of SPsynaptojanin. *B*, elimination of the inhibitory effect of Cu^{2+} by EDTA (*open circle*, Cu^{2+} alone; *solid triangle*, Cu^{2+} + 1 mM Mg^{2+}; *solid circle*, Cu^{2+} + 1 mM Mg^{2+} + 0.25 mM EDTA). The concentration of SPsynaptojanin was 4.4 nM, and the concentration of Ins(1,4,5)P_3 was 200 μM.

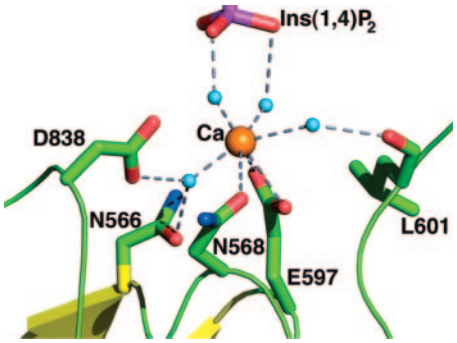

FIG. 6. **Calcium binding site in the SPsynaptojanin and Ins(1,4)P_2 complex.** Ca^{2+} (*orange sphere*) directly coordinates the carboxyl groups of Asn-568 and Glu-597 and water molecules (*cyan spheres*) that bind to Asn-566, Asp-838, the backbone oxygen of Leu-601, and the 4-phosphate of Ins(1,4)P_2.

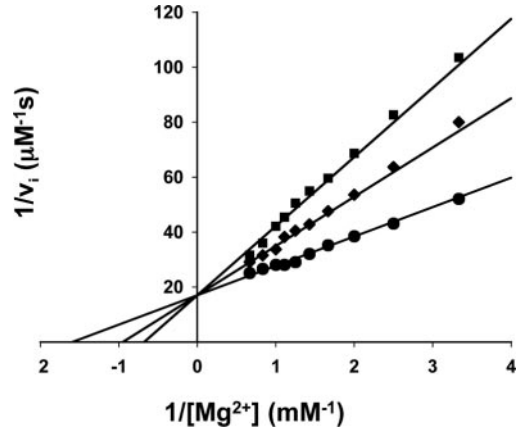

FIG. 7. **Inhibitory effect of Ca^{2+} on the catalytic activity of SPsynaptojanin.** The Ca^{2+} inhibition constant and its mode of inhibition were determined by varying the Mg^{2+} concentration at fixed levels of Ca^{2+}, 0 mM (*circle*), 0.5 mM (*diamond*), and 1.0 mM (*square*). Double-reciprocal plots for Ca^{2+} inhibition demonstrate that Ca^{2+} is a competitive inhibitor with respect to Mg^{2+} with a K_i value of 668 ± 78 μM.

Ins(1,4,5)P_3, Ins(1,3,4,5)P_4, and the lipids PtdIns(4,5)P_2 and PtdIns(3,4,5)P_3. We have shown that Ins(1,4,5)P_3 can serve as a very efficient substrate for SPsynaptojanin, with a substrate specificity constant (k_{cat}/K_m) of 2 × 10^5 $M^{-1}s^{-1}$. Interestingly, SPsynaptojanin displayed no measurable activity against α-D-glucose 1-phosphate, D-glucose 6-phosphate, or α-D,L-glycerophosphate. Most phosphatases, including the protein phosphatases, exhibit robust hydrolytic activity toward the highly activated substrates *p*-nitrophenyl phosphate and 3-*O*-methylfluorescein phosphate. The k_{cat} and K_m values for the SPsynaptojanin reactions are (4.04 ± 0.13) × 10^{-3} s^{-1} and 5860 ± 500 μM for *p*-nitrophenyl phosphate and (5.40 ± 0.30) × 10^{-4} s^{-1} and 182 ± 23 μM for 3-*O*-methylfluorescein phosphate at pH 7 and 30 °C. Thus, the k_{cat}/K_m values for *p*-nitrophenyl phosphate, 3-*O*-methylfluorescein phosphate, and other sugar phosphates are at least 5 orders of magnitude lower than that of Ins(1,4,5)P_3, a physiological substrate for SPsynaptojanin. Similar data were also obtained with the catalytic domain of human SHIP2. These results indicate that SPsynaptojanin and SHIP2 possess extremely high specificity for inositol phosphates.

To start to probe substrate specificity of SPsynaptojanin and SHIP2, we initially examined 8 commercially available inositol 5-phosphates, including 4 water-soluble inositol phosphates (Ins(1,5)P_2, Ins(1,3,5)P_3, Ins(1,4,5)P_3, and Ins(1,3,4,5)P_4) and four lipid inositol phosphates (diC$_4$PtdIns(5)P_1, diC$_4$PtdIns(3,5)P_2, diC$_4$PtdIns(4,5)P_2, and diC$_4$PtdIns(3,4,5)P_3), in which the fatty acid moieties are 4 carbons long to ensure aqueous solubility rather than 16, as they would be in cell membranes. As shown by the results summarized in Table II, SPsynaptojanin can dephosphorylate both water-soluble and lipid inositol phosphates. The hydrolyzes of Ins(1,4,5)P_3 and PtdIns(4,5)P_2 by SPsynaptojanin display similar catalytic efficiencies. The k_{cat}/K_m values for Ins(1,3,4,5)P_4 and PtdIns(3,4,5)P_3 are also similar, although they are 10-fold lower than those of Ins(1,4,5)P_3 and PtdIns(4,5)P_2, raising the possibility that the 3-phosphate may be inhibitory to SPsynaptojanin activity. Interestingly, although Ins(1,3,5)P_3 is not a substrate for SPsynaptojanin, PtdIns(3,5)P_2 is as good a substrate as PtdIns(3,4,5)P_3, suggesting that the lipid moieties can exert an effect on SPsynaptojanin activity. No activity was observed for SPsynaptojanin with Ins(1,5)P_2 and PtdIns(5)P_1 as substrates.

In contrast to SPsynaptojanin, SHIP2 is unable to dephosphorylate Ins(1,4,5)P_3 and PtdIns(4,5)P_2, whereas it is active toward both Ins(1,3,4,5)P_4 and PtdIns(3,4,5)P_4. This is consistent with the known preference of SHIP2 for 3-inositol phosphate substrates (3). Interestingly, the catalytic efficiency of SHIP2 toward Ins(1,3,4,5)P_4 is nearly 10-fold higher than its lipid derivative PtdIns(3,4,5)P_3. Similar to SPsynaptojanin, Ins(1,5)P_2 and PtdIns(5)P_1 cannot serve as substrates for SHIP2. Although SHIP2 could not utilize Ins(1,3,5)P_3 as a substrate, SHIP2 dephosphorylates PtdIns(3,5)P_2 as efficiently as PtdIns(3,4,5)P_3. Thus, contrary to the assumption that SHIP2 functions as a cellular PtdIns(3,4,5)P_3 phosphatase, SHIP2 can have additional water-soluble and lipid inositol phosphate substrates.

To gain further insights into the molecular determinants for SPsynaptojanin and SHIP2 substrate specificity, we decided to analyze additional inositol phosphates. There are 63 possible

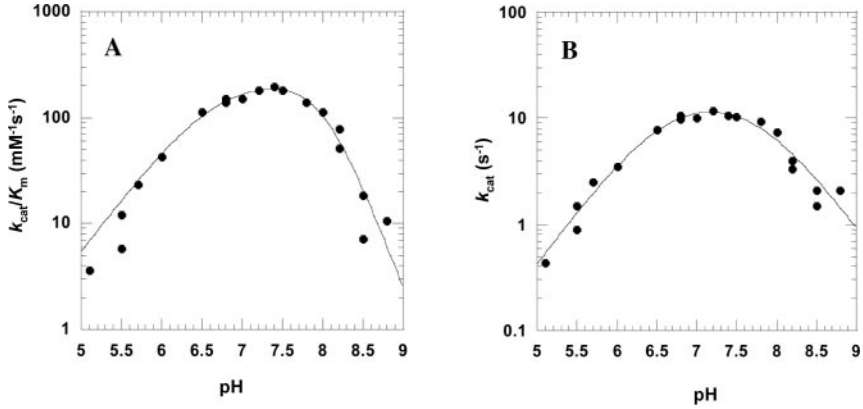

FIG. 8. **Effect of pH on k_{cat}/K_m (*A*) and k_{cat} (*B*) for the SPsynaptojanin-catalyzed dephosphorylation of Ins(1,4,5)P_3 at 1 mM Mg^{2+} concentration.** The catalytically essential ionization constants for the free enzyme and substrate were determined by fitting the data for k_{cat}/K_m *versus* pH to the equation $k_{cat}/K_m = (k_{cat}/K_m)^{max}/((1 + K_1/[H])(1 + [H]/K_2 + K_3/[H]))$. The catalytically essential ionization constants for the enzyme-substrate complex were determined by fitting the data for k_{cat} *versus* pH to the equation $k_{cat} = k_{cat}^{max}/(1 + [H]/K_1 + K_2/[H])$.

TABLE II
Substrate specificity of SPsynaptojanin and SHIP2 with eight commercially available inositol 5-phosphates

ND, not detectable.

Substrates	k_{cat}/K_m for SPsynaptojanin	k_{cat}/K_m for SHIP2
	$M^{-1}\,s^{-1}$	$M^{-1}\,s^{-1}$
Ins(1,4,5)P_3	$(2.08 \pm 0.04) \times 10^5$	ND
diC$_4$PtdIns(4,5)P_2	$(1.40 \pm 0.03) \times 10^5$	ND
Ins(1,3,4,5)P_4	$(8.78 \pm 0.05) \times 10^3$	$(9.60 \pm 0.60) \times 10^4$
diC$_4$PtdIns(3,4,5)P_3	$(1.30 \pm 0.02) \times 10^4$	$(1.01 \pm 0.01) \times 10^4$
Ins(1,3,5)P_3	ND	ND
diC$_4$PtdIns(3,5)P_2	$(1.88 \pm 0.02) \times 10^4$	$(1.15 \pm 0.16) \times 10^4$
Ins(1,5)P_2	ND	ND
diC$_4$PtdIns(5)P_1	ND	ND

TABLE III
Substrate specificity of SPsynaptojanin and SHIP2 with 54 water-soluble inositol phosphates

ND, not detectable.

Inositol 5-phosphates	k_{cat}/K_m for SPsynaptojanin	k_{cat}/K_m for SHIP2
	$M^{-1}\,s^{-1}$	$M^{-1}\,s^{-1}$
Ins(5)P_1	ND	ND
Ins(1,5)P_2	ND	ND
Ins(2,5)P_2	ND	ND
Ins(4,5)P_2	$(1.38 \pm 0.02) \times 10^5$	ND
Ins(1,2,5)P_3	ND	ND
Ins(1,3,5)P_3	ND	ND
Ins(2,3,5)P_3	ND	ND
Ins(1,4,5)P_3	$(2.08 \pm 0.04) \times 10^5$	ND
Ins(3,5,6)P_3	ND	ND
Ins(1,5,6)P_3	ND	ND
Ins(3,4,5)P_3	ND	ND
Ins(2,4,5)P_3	$(3.77 \pm 0.02) \times 10^6$	ND
Ins(2,5,6)P_3	ND	ND
Ins(4,5,6)P_3	$(7.90 \pm 0.01) \times 10^4$	ND
Ins(1,2,3,5)P_4	ND	ND
Ins(1,2,4,5)P_4	$(4.66 \pm 0.01) \times 10^4$	ND
Ins(2,3,5,6)P_4	ND	ND
Ins(1,2,5,6)P_4	ND	ND
Ins(2,3,4,5)P_4	ND	ND
Ins(1,3,4,5)P_4	$(8.78 \pm 0.05) \times 10^3$	$(9.60 \pm 0.60) \times 10^4$
Ins(1,3,5,6)P_4	ND	ND
Ins(1,4,5,6)P_4	ND	$(5.38 \pm 0.35) \times 10^3$
Ins(3,4,5,6)P_4	ND	ND
Ins(2,4,5,6)P_4	$(3.82 \pm 0.01) \times 10^4$	$(4.60 \pm 0.30) \times 10^3$
Ins(1,2,3,4,5)P_5	ND	$(7.80 \pm 0.78) \times 10^5$
Ins(1,2,3,5,6)P_5	ND	ND
Ins(1,2,4,5,6)P_5	$(2.49 \pm 0.02) \times 10^4$	ND
Ins(2,3,4,5,6)P_5	ND	ND
Ins(1,3,4,5,6)P_5	ND	ND

water-soluble inositol phosphates, whereas the upper limit for the lipid counterparts, in which only the 3-, 4-, and 5-hydroxyls are involved in generating isomers, is 7 (2). We examined all 4 possible isomers of lipid inositol molecules bearing a 5-phosphate (Table II). More structural variations are possible with water-soluble inositol phosphates. Indeed, more than 20 inositol phosphates have been identified in eukaryotic cells, many of which have not yet been assigned a function (28). In the following, we have determined the activity of SPsynaptojanin and SHIP2 toward 54 inositol phosphates.

Consistent with the assignment of SPsynaptojanin and SHIP2 as inositol-5-phosphatases, no activity was observed for the 25 inositol phosphates, which do not contain a phosphate at the 5 position: Ins(1)P_1, Ins(2)P_1, Ins(4)P_1, Ins(1,2)P_2, Ins(1,3)P_2, Ins(1,4)P_2, Ins(1,6)P_2, Ins(2,4)P_2, Ins(4,6)P_2, Ins(1,2,3)P_3, Ins(1,2,4)P_3, Ins(2,3,6)P_3, Ins(1,2,6)P_3, Ins(2,3,4)P_3, Ins(1,3,4)P_3, Ins(1,3,6)P_3, Ins(1,4,6)P_3, Ins(3,4,6)P_3, Ins(2,4,6)P_3, Ins(1,2,3,4)P_4, Ins(1,2,3,6)P_4, Ins(1,2,4,6)P_4, Ins(2,3,4,6)P_4, Ins(1,3,4,6)P_4, and Ins(1,2,3,4,6)P_5. Substrate specificity data for both SPsynaptojanin and SHIP2 with 29 inositol phosphates bearing a phosphate at the 5 position are summarized in Table III. Although SPsynaptojanin and SHIP2 are inositol-5-phosphatases, they display no detectable activity against Ins(5)P_1. Thus, efficient hydrolysis of the 5-phosphate moiety by SPsynaptojanin and SHIP2 may require optimal binding interactions between the active site residues and additional strategically positioned phosphate(s) on the inositol ring. Only a small subset of inositol polyphosphates can be efficiently processed by each enzyme (Table III).

For SPsynaptojanin, Ins(4,5)P_2, Ins(1,4,5)P_3, Ins(2,4,5)P_3, Ins(4,5,6)P_3, Ins(1,2,4,5)P_4, Ins(1,3,4,5)P_4, Ins(2,4,5,6)P_4, and Ins(1,2,4,5,6)P_5 were found to be excellent substrates with k_{cat}/K_m values in the range of 10^4–10^6 $M^{-1}s^{-1}$. Several conclusions are apparent upon examination of the results listed in Table III. The common structural feature for SPsynaptojanin substrates is the presence of a 4-phosphate in the inositol ring. Interestingly, the 4-phosphate in Ins(1,4)P_2, the hydrolysis product from Ins(1,4,5)P_3, was found in close proximity to the bound Ca^{2+} (Fig. 6 and Ref. 11). Our kinetic and mutagenesis data suggest that Mg^{2+} can also occupy the Ca^{2+} site, although the exact coordination spheres for the two metal ions may be different. We also found that Ins(1,4)P_2 is a competitive inhibitor of SPsynaptojanin with respect to Ins(1,4,5)P_3 (K_i = 306 ± 25 μM, data not shown). Thus, it is possible that the binding mode observed between the 4-phosphate group in Ins(1,4)P_2 and Ca^{2+} may be related to that between the 4-phosphate in the substrate and the Mg^{2+} cofactor. The interactions between the 4-phosphate in the substrate and the Mg^{2+} binding site in SPsynaptojanin may be essential to achieve precise transition state complementarity in the active site, accounting for the absolute requirement of 4-phosphate for SPsynaptojanin 5-phosphatase activity.

In the structural context of Ins(4,5)P_2, the presence of 1- (*i.e.* Ins(1,4,5)P_3) or 6-phosphate (*i.e.* Ins(4,5,6)P_3) appears inconsequential. However, introduction of a phosphate at the 3 position strongly hinders the reaction because no measurable activity was observed with Ins(3,4,5)P_3 as a substrate. To

ascertain whether the lack of activity for some of the 3-phosphate-containing inositols results from diminished binding, we determined the effect of Ins(3,5,6)P_3 on the SPsynaptojanin-catalyzed hydrolysis of Ins(1,4,5)P_3. The result shows that Ins(3,5,6)P_3 is a competitive and reversible inhibitor of SPsynaptojanin with a K_i of 22 ± 3 μM. Thus, the 3-phosphate-containing inositol Ins(3,5,6)P_3 is capable of binding to the active site of SPsynaptojanin even though it is not a substrate. Strikingly, we discovered that incorporation of a phosphate at the 2-position can further increase the k_{cat}/K_m for Ins(4,5)P_2 by more than 27-fold. This is due to a 3.9-fold increase in k_{cat} (41.2 ± 1.5 s^{-1} for Ins(2,4,5)P_3 and 10.5 ± 0.5 s^{-1} for Ins(4,5)P_2) and a 7-fold drop in K_m (10.9 ± 1.2 μM for Ins(2,4,5)P_3 and 75.9 ± 7.7 μM for Ins(4,5)P_2). The 2-hydroxyl group is axial to the plane of the inositol ring, whereas the remaining hydroxyls are all equatorial. This unique stereochemistry at the 2-position may allow additional contacts with the enzyme to further promote catalysis. Finally, SPsynaptojanin can also hydrolyze inositol tetrakisphosphates Ins(1,2,4,5)P_4, Ins(1,3,4,5)P_4, Ins(2,4,5,6)P_4, and inositol pentakisphosphate Ins(1,2,4,5,6)P_5, albeit with 4.5–24-fold lower k_{cat}/K_m values than that of Ins(1,4,5)P_3.

The substrate specificity for SHIP2 is more restricted than that of SPsynaptojanin. Unlike SPsynaptojanin, no significant activity was detected for SHIP2 with inositol phosphates having less than four phosphate groups. Only Ins(1,3,4,5)P_4, Ins(1,4,5,6)P_4, Ins(2,4,5,6)P_4, and Ins(1,2,3,4,5)P_5 were found to be excellent substrates for SHIP2 (Table III). Similar to SPsynaptojanin, in addition to the 5-phosphate, a common feature for the SHIP2 substrates is also the presence of a 4-phosphate group in the inositol ring. It is possible that the 4-phosphate group engages the catalytic machinery in SHIP2, including the Mg^{2+} binding site, in a manner similar to that proposed for SPsynaptojanin to promote SHIP2 catalysis. Surprisingly, in contrast to the notion that SHIP2 only hydrolyzes substrates with a 3-position phosphate group (3), both Ins(1,4,5,6)P_4 and Ins(2,4,5,6)P_4, inositol polyphosphates lacking a 3-phosphate, can also be effectively hydrolyzed by SHIP2. The best substrate identified for SHIP2 is inositol pentakisphosphate Ins(1,2,3,4,5)P_5, having a k_{cat}/K_m value that is 8-fold higher than that of Ins(1,3,4,5)P_4. Thus, the 2-position axial phosphate may have an activity enhancing effect on the SHIP2 reaction as well.

Conclusions and Biological Implications—We have established the regiospecificity for SPsynaptojanin. Using two non-radioactive spectroscopic assays we have characterized the metal ion and pH dependence of the SPsynaptojanin reaction. In addition to Mg^{2+}, transition metals such as Mn^{2+}, Co^{2+}, and Ni^{2+} are also effective in promoting SPsynaptojanin activity. In contrast, Ca^{2+} and Cu^{2+} are inhibitory. We provide evidence that Mg^{2+} occupies the same Ca^{2+} binding site observed in the crystal structure of the complex between SPsynaptojanin and Ins(1,4)P_2. The k_{cat}/K_m *versus* pH profile indicates that three ionizations of the free enzyme and/or free substrate are involved in the reaction of Ins(1,4,5)P_3; one group with a pK_a of 7.59 must deprotonated, and two groups with pK_a values of 6.66 and 8.41, must be protonated for optimal catalysis. The k_{cat} *versus* pH profile suggests that two groups in the enzyme-substrate complex are involved in catalysis; one group with a pK_a value of 6.60 must be deprotonated, and one group with a pK_a value of 7.75 must be protonated.

Substrate specificity analysis with four phosphatidylinositol phosphates bearing a 5-phosphate and 54 water-soluble inositol phosphates show that SPsynaptojanin and SHIP2 possess much broader substrate specificity than previously appreciated. In addition to the commonly accepted substrates PtdIns(4,5)P_2 and Ins(1,4,5)P_3, SPsynaptojanin can also dephosphorylate PtdIns(3,5)P_2, PtdIns(3,4,5)P_3, Ins(4,5)P_2, Ins(2,4,5)P_3, Ins(4,5,6)P_3, Ins(1,2,4,5)P_4, Ins(1,3,4,5)P_4, Ins(2,4,5,6)P_4, and Ins(1,2,4,5,6)P_5. Similarly, SHIP2 can hydrolyze PtdIns(3,5)P_2, Ins(1,4,5,6)P_4, Ins(2,4,5,6)P_4, and Ins(1,2,3,4,5)P_5 in addition to its known substrates Ins(1,3,4,5)P_4 and PtdIns(3,4,5)P. With the exception of PtdIns(3,5)P_2, all substrates contain a phosphate at the 4-position. The proximity of the 4-phosphate in the substrate to the Mg^{2+} coordination sphere may explain the dependence on 4-phosphate for the 5-phosphatase activity. The most efficient substrates for SPsynaptojanin and SHIP2 are Ins(2,4,5)P_3 and Ins(1,2,3,4,5)P_5, respectively, highlighting a novel activity enhancing property for the 2-phosphate. Although several inositol phosphates have clear functions *in vivo* (*e.g.* Ins(1,4,5)P_3 in Ca^{2+} influx and PtdIns(3,4,5)P_3 in activating the Akt/protein kinase B pathway), the exact roles of many others are continuously being defined. For example, both Ins(2,4,5)P_3 and Ins(1,3,4,5)P_4 have been proposed to potentiate the Ca^{2+}-mobilizing effects of Ins(1,4,5)P_3 and Ca^{2+} entry into cells (2, 27, 29, 30). Recent advances have revealed that several inositol polyphosphates ($InsP_4$, $InsP_5$, and $InsP_6$) can modulate the activities of chromatin-remodeling complexes (31, 32), and Ins(1,3,4,5,6)P_5 may serve as a proliferative signal (33). Given the fact that inositol phosphate isomers display different biological activities, the broad substrate specificity for SPsynaptojanin and SHIP2 suggest that these enzymes likely have additional roles in cell signaling and may regulate multiple distinct pathways. The unique substrate specificity profiles and the discovery that the 2-position is key to high affinity binding to SHIP2 have important implications for the design of potent and selective SHIP2 inhibitors for pharmacological investigation.

Acknowledgment—We thank Gali Prag for making Fig. 6.

REFERENCES

1. Anderson, R. A., Boronenkov, I. V., Doughman, S. D., Kunz, J., and Loijens, J. C. (1999) *J. Biol. Chem.* **274,** 9907–9910
2. Irvine, R. F., and Schell, M. (2001) *Nat. Rev. Mol. Cell Biol.* **2,** 327–338
3. Majerus, P. W., Kisseleva, M. V., and Norris, F. A. (1999) *J. Biol. Chem.* **274,** 10669–10672
4. Rameh, L. E., and Cantley, L. C. (1999) *J. Biol. Chem.* **274,** 8347–8350
5. Shears, S. B. (1998) *Biochim. Biophys. Acta* **1436,** 49–67
6. Maehama, T., Taylor, G. S., and Dixon, J. E. (2001) *Annu. Rev. Biochem.* **70,** 247–279
7. York, J. D., Ponder, J. W., and Majerus, P. W. (1995) *Proc. Natl. Acad. Sci. U. S. A.* **92,** 5149–5153
8. Zhang, Z.-Y. (2003) *Prog. Nucleic Acid Res. Mol. Biol.* **73,** 171–220
9. Norris, F. A., Atkins, R. C., and Majerus, P. W. (1997) *J. Biol. Chem.* **272,** 23859–23864
10. Erneux, C., Govaerts, C., Communi, D., and Pesesse, X. (1998) *Biochim. Biophys. Acta* **1436,** 185–199
11. Tsujishita, Y., Guo, S., Stolz, L. E., York, J. D., and Hurley, J. H. (2001) *Cell* **105,** 379–389
12. Cremona, O., Di Paolo, G., Wenk, M. R., Luthi, A., Kim, W. T., Takei, K., Daniell, L., Nemoto, Y., Shears, S. B., Flavell, R. A., McCormick, D. A., and De Camilli, P. (1999) *Cell* **99,** 179–188
13. Clement, S., Krause, U., Desmedt, F., Tanti, J. F., Behrends, J., Pesesse, X., Sasaki, T., Penninger, J., Doherty, M., Malaisse, W., Dumont, J. E., Le Marchand-Brustel, Y., Erneux, C., Hue, L., and Schurmans, S. (2001) *Nature* **409,** 92–97
14. Lin, T., Orrison, B. M., Leahey, A. M., Suchy, S. F., Bernard, D. J., Lewis, R. A., and Nussbaum, R. L. (1997) *Am. J. Hum. Genet.* **60,** 1384–1388
15. Chung, S. K., and Chang, Y. T. (1995) *J. Chem. Soc. Chem. Commun.* 11–12
16. Chung, S. K., and Chang, Y. T. (1996) *Kor. J. Med. Chem.* **6,** 162–165
17. Chung, S. K., and Chang, Y. T. (1996) *Bioorg. Med. Chem. Lett.* **6,** 2039–2042
18. Chung, S. K., Chang, Y. T., and Sohn, K. H. (1996) *J. Chem. Soc. Chem. Commun.* 163–164
19. Chung, S. K., Chang, Y. T., and Kwon, Y. U. (1998) *J. Carbohydr. Chem.* **17,** 369–384
20. Chung, S. K., Chang, Y. T., Lee, E. J., Shin, B. G., Kwon, Y. U., Kim, K. C., Lee, D. H., and Kim, M. J. (1998) *Bioorg. Med. Chem. Lett.* **8,** 1503–1506
21. Chung, S. K., Kwon, Y. U., Shin, J. H., Chang, Y. T., Lee, C., Shin, B. G., Kim, K. C., and Kim, M. J. (2002) *J. Org. Chem.* **67,** 5626–5637
22. McCain, D. F., and Zhang, Z.-Y. (2001) *Methods Enzymol.* **345,** 507–518
23. Webb, M. R. (1992) *Proc. Natl. Acad. Sci. U. S. A.* **89,** 4884–4887
24. Zhou, B., Wang, Z.-X., Zhao, Y., Brautigan, D. L., and Zhang, Z.-Y. (2002) *J. Biol. Chem.* **277,** 31818–31825
25. Cerdan, S., Hansen, C. A., Johanson, R., Inubushi, T., and Williamson, J. R. (1986) *J. Biol. Chem.* **261,** 14676–14680

26. Laxminarayan, K. M., Matzaris, M., Speed, C. J., and Mitchell, C. A. (1993) *J. Biol. Chem.* **268,** 4968–4974
27. Pattni, K., and Banting, G. (2004) *Cell. Signal.* **16,** 643–654
28. Majerus, P. W. (1992) *Annu. Rev. Biochem.* **61,** 225–250
29. Marchant, J. S., Chang, Y.-T., Chung, S. K., Irvine, R. F., and Taylor, C. W. (1997) *Biochem. J.* **321,** 573–576
30. Loomis-Husselbee, J. W., Walker, C. D., Bottomley, J. R., Cullen, P. J., Irvine, R. F., and Dawson, A. P. (1998) *Biochem. J.* **331,** 947–952
31. Shen, X., Xiao, H., Ranallo, R., Wu, W.-H., and Wu, C. (2003) *Science* **299,** 112–114
32. Steger, D. J., Haswell, E. S., Miller, A. L., Wente, S. R., and O'Shea, E. K. (2003) *Science* **299,** 114–116
33. Orchiston, E. A., Bennett, D., Leslie, N. R., Clarke, R. G., Winward, L., Downes, C. P., and Safrany, S. T. (2004) *J. Biol. Chem.* **279,** 1116–1122